Oxidation States of Copper Ions in ZSM-5 Zeolites. A Multitechnique Investigation

Gemma Turnes Palomino, Paola Fisicaro, Silvia Bordiga, and Adriano Zecchina

Dipartimento di Chimica IFM, Università di Torino, Via Giuria 7, 10125 Torino, Italy

Elio Giamello* and Carlo Lamberti

Dipartimento di Chimica IFM e Unità INFM di Torino, Via Giuria 9, 10125 Torino, Italy

Received: November 3, 1999; In Final Form: January 14, 2000

The redox behavior of Cu/ZSM-5 zeolites prepared by ion exchange from Cu^{2+} aqueous solutions has been followed by a variety of spectroscopic techniques to provide a thorough picture of the so-called "self-reduction" of cupric ions, which occurs upon dehydration of the hydrated system at various temperatures, and of the reverse process of reoxidation as well. Conflicting hypotheses on both these processes are, in fact, present in the literature. The experimental techniques employed in this work are electron paramagnetic resonance (EPR), IR, and optical spectroscopies, extended X-ray absorption fine structure, and X-ray absorption near-edge structure. The early stages of dehydration (from room temperature to about 470 K) involve cupric ion migration and formation of EPR silent moieties but no reduction to Cu^{+}. The onset of this latter phenomenon starts at 470 K and, in the range 470−670 K, involves the majority of copper ions present in the system. Rehydration of Cu^{+}-containing samples does not cause direct Cu^{+} oxidation to Cu^{2+} but favor this latter process when O_2 is used as oxidant. Oxidation of Cu^{+} to Cu^{2+} by molecular oxygen, in fact, does not take place at room temperature if O_2 is contacted with the dehydrated material but easily occurs when oxygen is adsorbed on rehydrated samples at the same temperature.

1. Introduction

Copper ion exchanged molecular sieves have been widely investigated in the past to characterize the location, coordination state, adsorptive capacity, reactivity and mobility of metal ions in the frame of various zeolites by means of a variety of experimental techniques.[1−4] More recently, after the discovery that copper exchanged ZSM-5 zeolites are active in the direct decomposition of nitric oxide to nitrogen and oxygen,[5−9] a new set of studies on the chemistry of copper in this and other zeolites has been undertaken. The aim of this intense activity is to describe the nature of the active site, the physicochemical conditions to form the maximum amount of such sites, and the molecular mechanism of the catalytic decomposition. Besides the classic techniques of molecular spectroscopy (UV−vis, infrared), magnetic resonance (electron paramagnetic resonance, EPR), thermogravimetry, and adsorption, the X-ray absorption fine structure (XAFS) spectroscopy has played an important role in the recent experimental activity mainly to identify the nature of copper ions and to describe their local environment.[10−18]

However, despite the great deal of investigation in the field, some problems of vital importance to understand the Cu/ZSM-5 catalytic system are still discussed in the literature. One of the most debated problems concerns the oxidation state of copper in various conditions or, in other words, the whole redox chemistry of copper in the zeolitic framework. Solving this problem is essential to define the nature of the copper centers present in various conditions in the working catalyst and is therefore preliminary to the other, highly debated, problem of the catalytic reaction mechanism. Many authors have reported, for instance, that upon treatment under vacuum (or in a flow of inert gas) at moderate temperature of samples containing hydrated cupric Cu^{2+} ions a substantial fraction of these ions are reduced to Cu^{+}.[19−24] To explain this fact, often called "self-reduction" of Cu^{2+}, two chemical pathways are discussed in the literature. The first mechanism involves the loss of both water and oxygen according to the following equation: where

$$2[CuOH]^{+} \leftrightarrow Cu^{2+}O^{2-}Cu^{2+} + H_2O \leftrightarrow Cu^{+}\square Cu^{+} + {}^{1}/_{2}O_2 \quad (1)$$

the starting cupric ions are written in the hydroxylated form present in hydrated zeolites (as pointed out by Iwamoto and co-workers[5−9]) and the symbol □ represents a vacancy of an "extralattice oxygen" (formed by condensation of two OH groups and thus introduced in the zeolite along the ion exchange process) since no oxygen can be depleted from the zeolitic framework. The extralattice oxygen (ELO) is eliminated, by desorption of O_2 (as indicated in eq 1). Keith Hall and co-workers[23] discussed the phenomenon in terms of the sublimation pressure of O_2 with consequent formation of Cu^{+} ions and assigned a low-frequency IR band (910 cm^{-1}) to the ELO species. The second mechanism, exclusively based on water elimination, has been proposed quite recently by Bell and co-workers on the basis of EPR data and is based on a complex pathway involving formation of hydroxyl radical ($OH^{\bullet}$) and O^{-} ions:[25]

$$Cu^{2+}OH^{-} \leftrightarrow Cu^{+} + OH^{\bullet} \quad (2)$$

$$Cu^{2+}OH^{-} + OH^{\bullet} \leftrightarrow Cu^{2+}O^{-} + H_2O \quad (3)$$

$$2[Cu^{2+}OH^{-}] \leftrightarrow Cu^{+} + Cu^{2+}O^{-} + H_2O \quad (4)$$

According to this mechanism a fraction of copper is actually reduced to Cu^{+} but a second fraction remains as Cu^{2+} under

* To whom correspondence should be addressed. E-mail: Giamello@ch.unito.it.

10.1021/jp993893u CCC: $19.00
Published on Web 03/30/2000

the form of a $Cu^{2+}O^-$ pair, undetectable by EPR (eq 4). The addition of water, in this case, restores the initial oxidation state without any need of molecular oxygen. The above mechanism has been proposed essentially on the basis of the fact that the intensity of Cu^{2+} EPR spectra drops out upon thermal treatment in vacuo and is restored by simple water adsorption at room temperature. The hypothesis and mechanism reported above were contrasted by LoJacono, Keith Hall, and co-workers,[26] who suggested, on the basis of magnetic susceptibility measurements, that the loss of intensity of the EPR signal between room temperature and 473 K is not due to reduction of cupric ions to Cu^+ but to changes in the coordination of Cu^{2+} ions which become EPR inactive even without reduction. The effect of reoxidation by water, postulated by Bell (eq 2), should be just a recovery of the original water coordination (and of the EPR signal as well) of the cupric ions.

The aim of the present paper is to attempt an overall description of the redox chemistry of copper in ZSM-5 zeolites prepared by ion exchange in aqueous solution, analyzing both the dehydration−thermal reduction process of cupric ions in the range between room temperature and 673 K (i.e., in a range of temperature of interest for the catalytic decomposition of NO) and the reverse process in various conditions. In particular we will examine in detail the reoxidation by O_2 at various temperatures and hydration states of the solid and the role of water in the reoxidation process. To accomplish this task, a set of complementary spectroscopic techniques have been used and the respective results compared one with each other. The present investigation on solution exchanged Cu/ZSM-5 parallels previous work from our laboratory on the Cu/ZSM-5 system prepared via gas-phase exchange with CuCl and whose chemistry was followed by the same techniques adopted here.[17]

2. Experimental Section

A H-ZSM-5 sample ($SiO_2/Al_2O_3 = 28$), kindly supplied by Enichem SpA, Centro Ricerche Novara, has been used. The copper ion exchange was carried out by stirring the H-ZSM-5 sample in a 0.4 M $Cu(NO_3)_2$ solution at room temperature for 3 days. This procedure was repeated two times. The extent of ion exchange (∼80%) was approximately evaluated by comparison of the intensity of the band at 3610 cm^{-1}, characteristic of the O−H stretching mode of framework −Al(OH)Si− groups, before and after the exchange.

X band EPR spectra of Cu^{2+} were run at 77 K on a Varian E-109 spectrometer equipped with a dual cavity always employing the same set of instrumental parameters. The sample was contained in a quartz cell designed to allow in situ thermal treatments, gas adsorption, and spectrum recording.

Double integration of each spectrum was performed to follow the evolution of the amount of EPR visible Cu^{2+} ions along the various treatments. Since the highest recorded intensity in each experiment is that of the as-prepared hydrated material, this latter one is indicated with 1.0 in the quantitative plots, and all other intensities, recorded in various conditions, are referred to this value.

For IR measurements, a thin self-supporting wafer of the zeolite was prepared and activated under dynamic vacuum at increasing temperatures, 300, 373, 473, 573, and 673 K, for 2 h, inside an IR cell designed to allow in situ high-temperature treatments, gas dosage, and low-temperature measurements. The IR spectra were recorded at 2 cm^{-1} resolution on a BRUKER FTIR 66 spectrometer equipped with a mercury−cadmium−telluride (MCT) cryodetector. Vis−near-IR diffuse reflectance experiments have been performed with a Varian CARY5 spectrophotometer.

An X-ray absorption experiment has been performed at the GILDA MB8 beamline[27] at the European Synchrotron Radiation Facility (ESRF) during experiment CH-542.[28] The monochromator was equipped with two Si(311) crystals while harmonic rejection was achieved using mirrors. To ensure very high quality X-ray absorption near-edge structure (XANES) spectra, the geometry of the beamline was optimized to improve the energy resolution: vertical slits, located 23 m from the source, were set to 0.6 mm, ensuring at 9 keV an actual energy resolution better than 0.5 eV. The following experimental geometry was adopted: (1) I_0 (1 bar of N_2 filled ionization detector having an efficiency of 10%); (2) zeolite sample; (3) I_1 (100 mbar of Ar filled ionization detector having an efficiency of 50%); (4) 7 μm thick copper metal foil; (5) I_2 (photodetector). This setup allows a direct energy/angle calibration for each spectrum, avoiding any problem related to small energy shifts due to small thermal instability of the monochromator crystals (phenomenon particularly critical after each injection). The first maximum of the XANES derivative spectrum of the Cu metal foil (corresponding to the 1s → 4p electronic transition of Cu^0) has been defined as 9879.0 eV. The stability of the beamline was excellent, since successive acquisitions have shown a shift of the copper metal 1s → 4p peak within ±0.2 eV (vide infra, bottom inset of Figure 3A. This shift reaches a typical value of 0.5 eV after injection. This experimental geometry implies that the dynamical focusing mode, available at the GILDA BM8 beamline,[27] has not been used.

A sampling step of 0.2 eV for the XANES part of the spectra and a variable sampling step, giving $\Delta k_{max} = 0.05$ Å^{-1} for the EXAFS part, and an integration time of 3 s/point have been adopted. Spectra were collected at room temperature (RT) using a metallic cell, allowing in situ treatments up to 800 K and gas dosage.

The following procedures have been adopted: Cu^{2+}/ZSM-5 has been activated under dynamic vacuum at increasing temperatures, 300, 373, 473, 573, and 673 K, for 2 h, and three equivalent XANES and EXAFS spectra have been collected between each activation step. The sample activated at 673 K has been exposed to the vapor pressure of H_2O at room temperature for about 2 h; after EXAFS measurements O_2 has been admitted (100 Torr of equilibrium pressure) on the hydrated sample, and a second EXAFS experiment was run.

For each sample three equivalent spectra have been collected, and extracted $\chi(k)$ values have been averaged before the EXAFS data analysis. The standard deviation calculated from the averaged spectra was used as an estimate of the statistical noise for the evaluation of the error associated with each structural parameter. The EXAFS data analysis has been performed following standard procedures.[29] Experimental $\chi(k)$ was extracted from absorption data by a conventional procedure outlined as follows: a linear background was fitted in the preedge region, extrapolated to higher energies, and then subtracted from absorption data. An atomic-like contribution was estimated by a polynomial fit of fifth degree and then subtracted from experimental data following the procedure proposed by Lengeler and Eisenberger.[30] The result was normalized to edge height to obtain experimental $\chi(k)$ values. The k^3-weighted $\chi(k)$ values were Fourier transformed over a Kaiser window, with $\tau = 2.5$, in the range 3.6−13.9 Å^{-1}. Main contributions to the Fourier transform modulus were filtered to obtain the Cu nearest-neighbor shell in the 1.1−2.0 Å interval ($2\Delta k\Delta r/\pi \approx 5.9$). The so-obtained filtered contributions were analyzed using the programs developed by Michalowicz.[31] The EXAFS results have been obtained by extracting the experi-

mental phase shift and amplitude functions from the model compound Cu_2O.

3. Results and Discussion

3.1. Thermal Reduction of Cu^{2+}/ZSM-5 under Vacuum. The modifications of the hydrated system upon dehydrating in vacuo at increasing temperature have been followed by a variety of experimental techniques including EPR, IR absorption due to skeletal vibrations and to adsorbed molecules, vis−near-IR, and XAFS. Due to the controversial conclusions present in the literature about EPR data (spectra of Cu^{2+} ions) these latter ones will be presented first.

3.1.1. EPR Spectroscopy. Cu^{2+} ions are $3d^9$ paramagnetic ions and, as reported in the Introduction, are easily observed by EPR. Cu^+ ions, on the contrary, are diamagnetic ($3d^{10}$) and therefore EPR silent.

All the reported EPR spectra of Cu^{2+} in zeolites are basically not different from the vaste majority of the spectra of cupric ions in molecular and solid-state compounds, which usually contain Cu^{2+} in variously distorted octahedral or square planar symmetries. The spin-Hamiltonian parameters in such cases have axial structure ($g_{xx} = g_{yy} = g_\perp$; $g_{zz} = g_{||}$). The g values are higher than the free spin value ($g_e = 2.0023$) with the sequence $g_{||} > g_\perp > g_e$, and the hyperfine coupling tensor, due to the $I = 3/2$ nuclear spin of ^{63}Cu and ^{65}Cu which splits each resonance in four lines, has the structure $A_{||} > A_\perp$. The spin-Hamiltonian parameters of cupric ions in ZSM-5 are well-known[32−36] and have also been reported in previous work from our laboratory.[17,35,36] They will not therefore be deeply discussed in the present paper, which devotes a particular attention to the intensity variations of the spectra to get information on the redox chemistry of the systems.

The "as-prepared" materials after exchange have an EPR spectrum typical of hydrated copper ions which, when recorded at 77 K, exhibits a broad axial signal with scarcely resolved parallel hyperfine structure (figure not reported). The same spectrum recorded at room temperature tends to be isotropic and less resolved, indicating a partial mobility of the hydrated cupric species.

The effect of treating the samples under vacuum and at increasing temperature is well-known and consists of the loss of spectral intensity and in the increase of resolution as shown in Figure 1A. Due to the low concentration of cupric species the final spectrum is well resolved also in the perpendicular component. As already remarked by Larsen[25] et al. and by Lo Jacono et al.,[26] the intensity decrease is not progressive, and usually at temperatures higher than 570 K, some oscillation in the intensity values is observed with increasing temperature as shown in Figure 1B, which reports the spectral intensity observed after steps of 30′ thermovacuum treatment in the range between 300 and 670 K. The intensities reported in Figure 1B are in arbitrary units, and the intensity 1 is conventionally attributed to the starting sample (brief evacuation at room temperature). Despite the mentioned dumping (which will be discussed in the following), the spectral intensity is reduced to few percents of its initial value. The phenomenon is always observed even though the exact trend of the intensity plot is not perfectly reproducible from one experiment to the other.

3.1.2. Infrared and Vis−Near-IR Spectroscopies. The infrared spectrum of zeolitic materials with MFI structure in the 1300−800 cm^{-1} range is dominated by the high-intensity ν_{asym}(SiOSi) modes absorbing in the 1350−1000 cm^{-1} interval and by the ν_{sym}(SiOSi) modes in the 850−700 cm^{-1} region. It has been shown that in some cases the presence in the framework of a small concentration of heteroatoms (both framework and extraframework) is sufficient to induce well-defined and typical bands in the "transmission window" between these absorptions. In few cases these new bands are even used as a fingerprint of the material. This is the case of the band at 960 cm^{-1} of TS-1[37,38] or of the band at 1006 cm^{-1} for Fe−Silicalite.[37,39] Analogue manifestations, around 900 cm^{-1}, have also been observed in the case of divalent metal-exchanged zeolites.[40−43] These latter absorptions can be assigned to ν_{asym}(SiOAl) modes perturbed by extraframework cations $(M)^{2+}$. Two parameters play a role in determining the frequency and the intensity of these bands: the mass of the extraframework species and the force constant of the $O-M^{n+}$ bond, the last being influenced by the charge of the ion and by the number and type of the ligands in the coordination sphere.

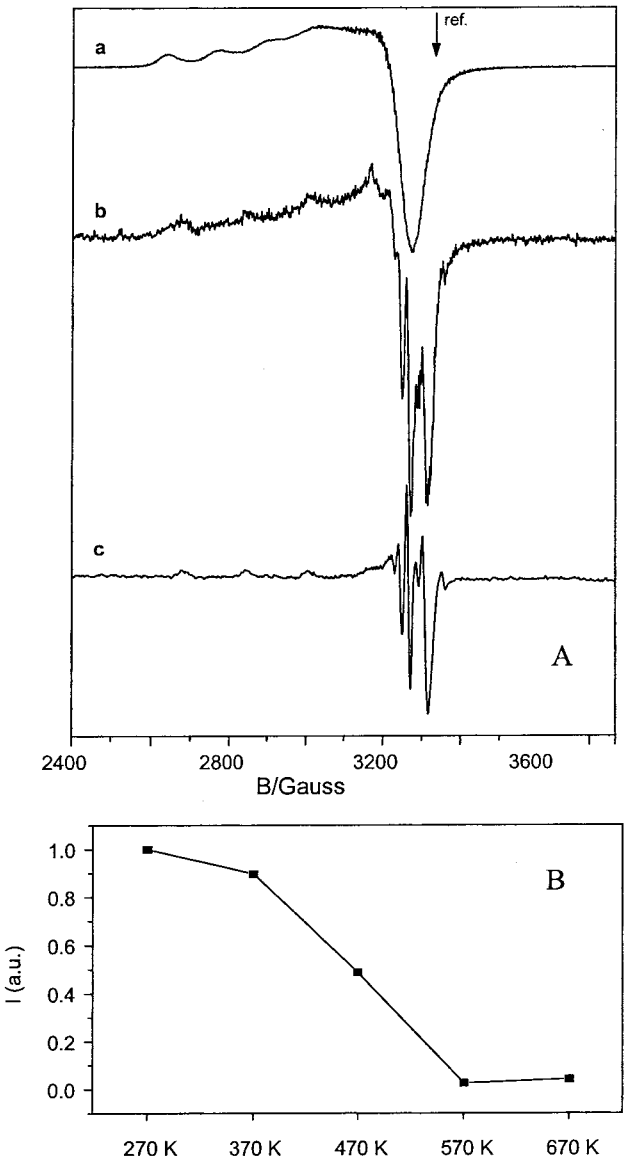

Figure 1. (A) EPR spectra of Cu/ZSM-5 dehydrated under vacuum at increasing temperature. (B) Intensity of EPR spectra as a function of dehydration temperature. In part A spectra recorded at 77 K after treatment at room temperature (a), 473 K (b), and 673 K (c), respectively, are reported.

Coming now to the copper exchanged system,[41−43] a different spectroscopic manifestation is, in principle, expected for cuprous and cupric ions so that the transformation of Cu^{2+} into Cu^+ should be accompanied by substantial changes of the bands in the 1000−800 cm^{-1} range. In Figure 2A the effect of thermal

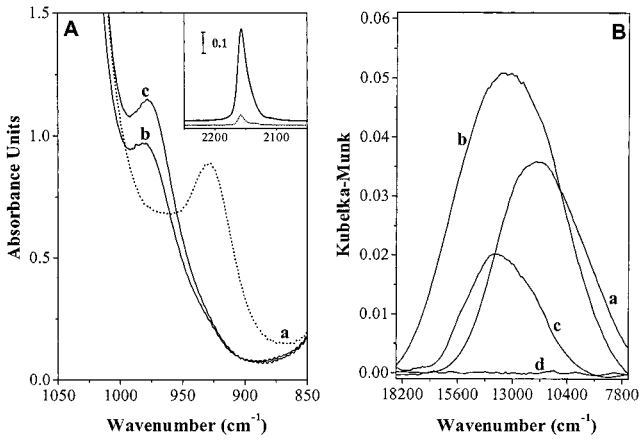

Figure 2. (A) Evolution of the IR spectra in the 1050−850 cm^{-1} range upon thermal treatment activation of the sample at 373, 473, and 673 K: curves a, b, and c, respectively. The inset shows, in the CO stretching region, the band due to the $Cu^{+}\cdots CO$ adduct obtained by dosing CO on the sample activated at 373 and 673 K: dotted and full lines, respectively. (B) Evolution of the vis−near-IR spectra, in the d−d region, upon thermal treatment activation of the sample at 300, 373, 473, and 673 K: curves a−d.

treatment at various temperatures on Cu^{2+} exchanged ZSM-5 is reported. Spectrum a, obtained after activation at 373 K, shows a band at 920 cm^{-1} which is ascribed to a ν_{asym}(SiOAl) perturbed by Cu^{2+} ions; upon thermal treatment at 473 and 673 K, this band is gradually transformed into a new component at 980 cm^{-1}, which is associated with the Cu^{+} species. The nearly complete disappearance of the band at 920 cm^{-1} indicates that, at this temperature, a substantial reduction of Cu^{2+} into Cu^{+} has occurred.

The progressive reduction of Cu^{2+} into Cu^{+} species upon thermal treatment in vacuo can also be probed by CO adsorption. Carbon monoxide is a weak Lewis base that interacts with coordinatively unsaturated centers, forming pure σ-complexes (in d^0 systems) and σ,π-complexes (in d^n systems). When CO uptake is carried out at low temperatures (e.g., at liquid nitrogen temperature), the reducing activity of CO observed at room temperature is inhibited and the interactions of the acid−base type only may occur. In such conditions it is well-known that CO forms stable carbonyls with coordinatively unsaturated Cu^{+} while it does not coordinate on cupric ions. In the inset of Figure 2A the IR spectra recorded at low temperature for the interaction of CO with Cu/ZSM-5 samples treated in vacuo at stepwise increasing temperature are reported. An absorption band at $\nu \approx 2157$ cm^{-1}, due to CO coordinated on Cu^{+} ions, arises starting from 470 K dehydration temperature and reaches its maximum intensity for samples treated at 570 K. This experiment again shows that cuprous ions are actually formed along thermo-vacuum treatment of the sample. The growth of the CO infrared band however does not exactly parallel the loss of EPR intensity shown in Figure 1B in that the loss of Cu^{2+} intensity starts with the initial stages of the dehydration while the evidence of Cu^{+}−CO coordination appears at higher temperature.

The UV−vis spectroscopy of Cu^{2+} ion differs from that of Cu^{+} because the latter has a closed shell configuration, while the former has an incomplete d shell configuration. This implies that a sample exchanged with Cu^{+} is colorless (no d−d transition being expected), while a sample containing Cu^{2+} species is colored (because of the presence of the typical d−d transitions). In Figure 2B the spectra obtained on the untreated Cu^{2+}/ZSM-5 sample (thus containing adsorbed water) and after subsequent outgassing at 373, 473, and 673 K are reported. The freshly prepared sample shows a broad absorption centered at 12.500 cm^{-1} characteristic of Cu^{2+} hydrated species.[44] Upon outgassing treatment at 373 K a shift of the band at higher frequency with intensification is observed. Thermal treatment at higher temperature causes a progressive erosion of the band which practically disappears after outgassing at 673 K, indicating the progressive transformation of Cu^{2+} into Cu^{+} species.

The absorption at 12.500 cm^{-1} is easily assigned to a spin-allowed transition ^2E_g- - -^2T_g for Cu^{2+} species in octahedral coordination, such as $Cu^{2+}(H_2O)_6$, as documented by literature data available for homogeneous complexes,[44,45] and for solid solution of Cu^{2+} in Al_2O_3.[46] The shift to higher frequency and the intensity increase observed upon thermal treatment at 100 °C are due to water removal which forces Cu^{2+} species to interact with the oxygens of the zeolitic framework. Under this condition the local symmetry of Cu^{2+} becomes lower than octahedral, explaining the observed spectral behavior in analogy with that found for homogeneous complexes.[45]

3.1.3. XAFS. Due to the atomic selectivity and sensitivity to both local environment and oxidation state of the selected atomic species typical of EXAFS and XANES, several groups have used these techniques to characterize the oxidation and aggregation states of copper species in zeolites in various conditions and after interaction with adsorbates (see for instance refs 10−18 for Cu/ZSM-5).

In fact, the preedge region of X-ray absorption spectra provides direct information on the oxidation state of copper.[47−50] It is widely recognized that a single well-defined peak at 8983−8984 eV is the fingerprint of Cu^{+} species. This peak is due to the dipole-allowed 1s → 4p electronic transition of Cu(I). On the contrary, Cu^{2+} species exhibit (i) a weak absorption at about 8976−8979 eV, attributed to the dipole-forbidden 1s → 3d electronic transition and (ii) a shoulder at about 8985−8988 eV and an intense peak at about 8995−8998 eV, both due to 1s → 4p transitions.

Because of the great differences between the preedge spectra of Cu^{+} and Cu^{2+} ions, we decided to follow the thermal reduction of a Cu/ZSM-5 sample with XANES spectroscopy and to try to evaluate the degree of subsequent oxidation by in situ interaction with H_2O and H_2O/O_2 mixtures.

Figure 3A reports the XANES spectra collected on the Cu/ZSM-5 sample activated at increasing temperatures. A progressive red shift of the adsorption edge is evident, together with the parallel appearance of the strong preedge peak, due to the dipole-allowed 1s → 4p transition of Cu^{+} ions, in the 8983 eV range. As a minor feature, magnified in the inset, also the progressive erosion of the weak 1s → 3d absorption at about 8977.5 eV has been observed. All these results are clear evidence that the $Cu^{2+} \rightarrow Cu^{+}$ thermal reduction is very extended for sample activated at 673 K. Similar data have been reported by Kuroda et al. on Cu^{2+}-containing mordenite[51,52] and, very recently, also on Cu/ZSM-5.[18] In this latter case the fraction of thermally reduced Cu^{+} species has been evaluated, by comparison with XANES spectra of model compounds, and reaches a value of 0.70 upon activation at 873 K.[18]

The parallel EXAFS data are reported in Figure 3B. Corresponding k^3-weighted Fourier transform (FT) data are reported in Figure 4. A simple inspection of the raw EXAFS data reported in Figure 3B indicates a strong reduction of the $\chi(k)$ oscillations, reflecting a decrease of the first shell coordination number of copper species during the $Cu^{2+} \rightarrow Cu^{+}$ thermal reduction. The same conclusion is reached by considering the corresponding FT reported in Figure 4 where the reduction of the first shell Cu−O peak is evident. Quantitative EXAFS analysis indicates a dramatic reduction of the Cu−O coordination number from

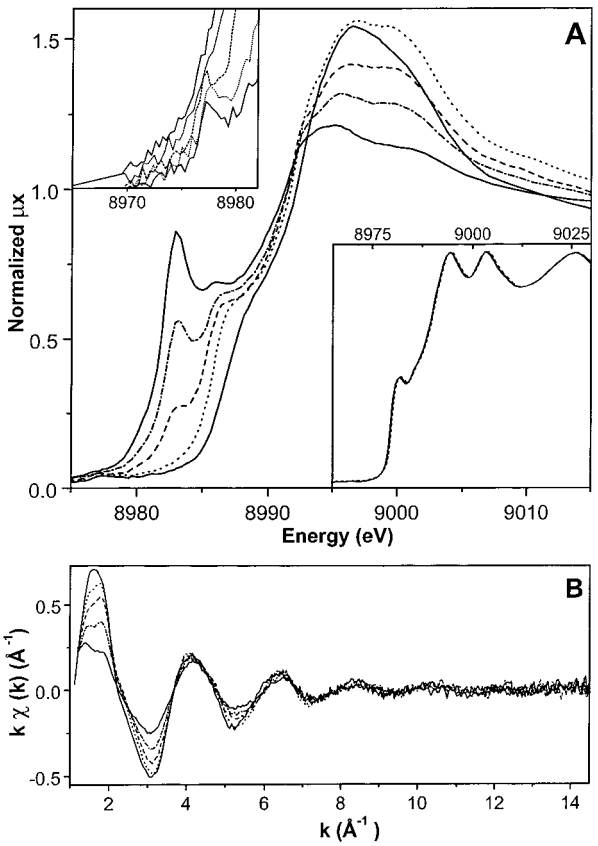

Figure 3. (A) XANES spectra of Cu^{II}/ZSM-5 thermally treated at increasing temperatures: 300 K (full line), 373 K (dotted line), 473 K (dashed line), 573 K (dotted−dashed line), and 673 K (full line again). The inset in the upper left corner reports the magnification of the 1s → 3d electronic transition, while the inset in the lower right corner reports the five superimposed XANES spectra of the Cu reference foil collected simultaneously with the XANES spectra of the Cu^{II}/ZSM-5 sample. (B) As part A for the experimental $k\chi(k)$ spectra (averaged over three acquisitions).

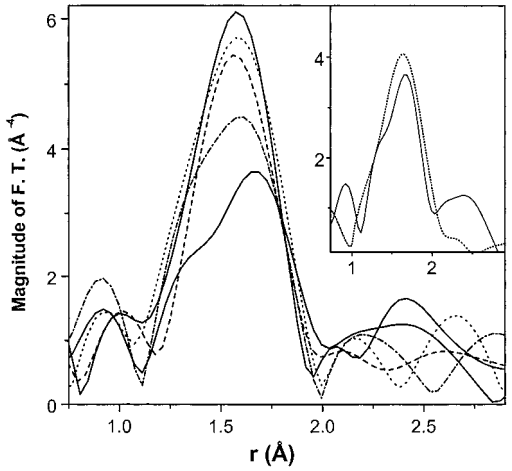

Figure 4. k^3-weighted FT of EXAFS data reported in Figure 3B (lines with the same drafts in Figure 3B). The inset reports the comparison between Cu^{II}/ZSM-5 thermally activated at 673 K (full line) and Cu^{I}/ZSM-5 prepared from CuCl (dotted line, taken from ref 17).

3.9 ± 0.4 to 2.3 ± 0.3 correlated with a small increment of the first shell Cu−O distance (from 1.94 ± 0.02 to 1.98 ± 0.02 Å), due to the higher ionic radius of Cu^+ with respect to Cu^{2+}. A similar result was obtained by Kuroda and co-workers for the thermal reduction of Cu^{2+}−Mordenite[51,52] where the coordination number (and the Cu−O distance) moves from 4.2 (1.95 Å) to 3.1 (1.98 Å) for Cu^{2+}−Mordenite activated at 300 and 673 K, respectively, reaching a value of 2.5 (2.02 Å) for the sample activated at 873 K. For the sake of comparison, it is also worth underlining that the average Cu^+ first coordination shell of Cu^{2+}/ZSM-5 thermally activated at 673 K is similar to that of Cu^+/ZSM-5 prepared by gas-phase reaction with CuCl:[17] $N = 2.5 \pm 0.3$; $r = 2.00 \pm 0.02$ Å; $\sigma = 0.073 \pm 0.010$ Å. This fact is clearly visible in the inset of Figure 3A, where the k^3-weighted FT of the Cu^{2+}/ZSM-5 sample activated at 673 K (full line) is reported together with the same FT of Cu^+/ZSM-5 prepared from CuCl. The second shell contribution of the two samples, however, is totally different. Cu^+/ZSM-5 prepared from CuCl, in fact, does not show any significant higher shell contribution, confirming that it contains isolated Cu^+ species,[17] whereas the Cu^{2+}/ZSM-5 sample activated at 673 K clearly shows (Figure 4) a consistent contribution at about 2.4 Å (without any phase correction): such a signal has already been observed by several authors in Cu zeolites prepared from the conventional liquid exchange with Cu^{2+} salts and attributed to Cu−O−Cu dimeric oxocations.[16,51−56]

In conclusion, the progressive dehydration of the system at increasing temperature is accompanied by the progressive reduction of the cupric ions to cuprous ions. The process starts at about 473 K and reach its maximum extension at about 673 K. The remarkable decrease of the EPR signal at a dehydration temperature lower than 473 K does not involve copper ion reduction, as indicated by Lo Jacono et al.[26] in contrast with the ideas of Larsen et al.[25] A detailed description of the reductive process will be reported in section 3.3 of the present paper.

3.2. Reoxidation of Dehydrated Reduced Samples. *3.2.1. EPR Spectroscopy.* Contacting a sample thermally treated in vacuo at 673 K with oxygen at ambient temperature, no variation in the EPR spectrum is observed. Upon increasing the temperature under oxygen atmosphere the intensity of the EPR spectrum increases starting from 373 K as shown in Figure 5 and reaches a maximum value for oxidation at 673 K. In these conditions a second Cu^{2+} species is present in the system besides the main species observed on dehydrated samples. The intensity increase upon oxidation is reported in Figure 5B, from which it can be assumed that the final intensity after oxidation at 673 K is about 40% of the original intensity of the hydrated as-prepared material. Adsorption of water after reoxidation in O_2 causes the evolution of the spectrum containing the two isolated Cu^{2+} species, which assumes the typical shape of hydrated cupric complexes similar to that in Figure 1A (spectrum a) and is accompanied by a further growth of the spectral intensity, which becomes close to that of the original sample.

Differently from the effect of oxygen, water vapor adsorption at room temperature onto dehydrated samples causes a remarkable increase of the EPR intensity. The phenomenon is time and pressure dependent. The effect of increasing doses of water (always kept in equilibrium with the solid for 1 min, except differently reported) on the EPR spectrum is reported in Figure 6. The spectra after contact with water assume the typical shape and parameters due to water cupric complexes (Figure 1a) and increase in intensity by increasing the water uptake as shown by spectrum d in Figure 6 recorded after 2 h of contact with water. The quantitative values are shown in Figure 6B (first four spectra), which indicates that (upon rehydration at room temperature) the EPR intensity increases up to about 30 times that of the dehydrated starting sample (first spectrum), reaching a value that is about 40% of the reference value typical of starting materials.

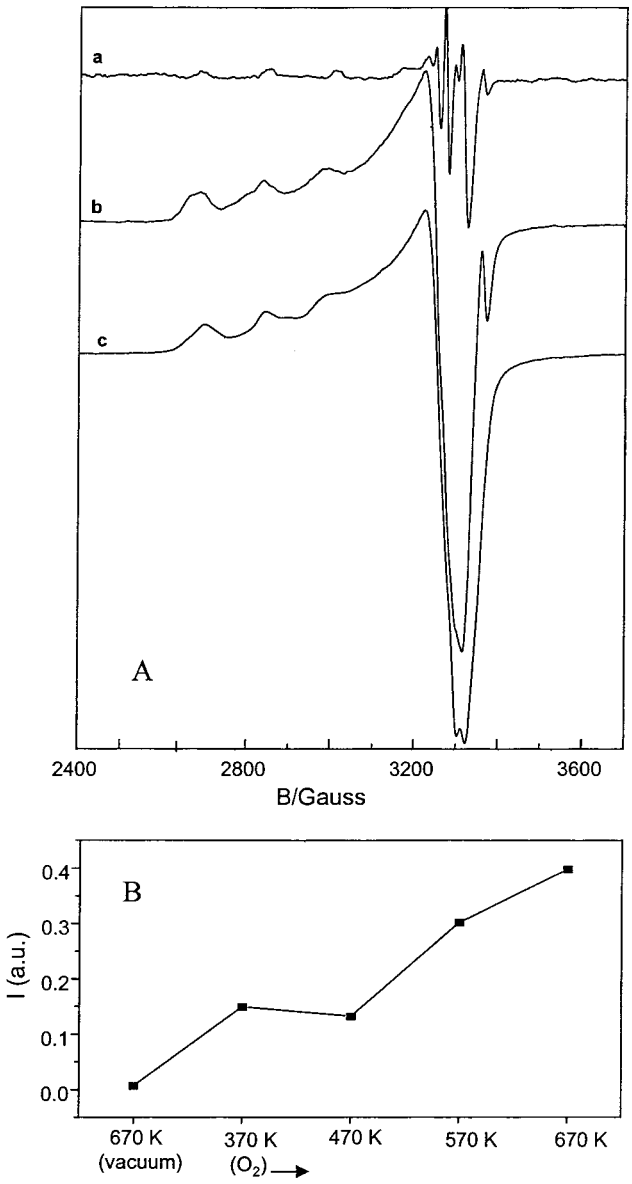

Figure 5. EPR spectra (A) and corresponding intensities (B) of Cu/ZSM-5 in dry oxygen at increasing temperature. In Part A the spectra after outgassing at 673 K (a) and oxidation at 473 K (b) and 673 K (c) are reported.

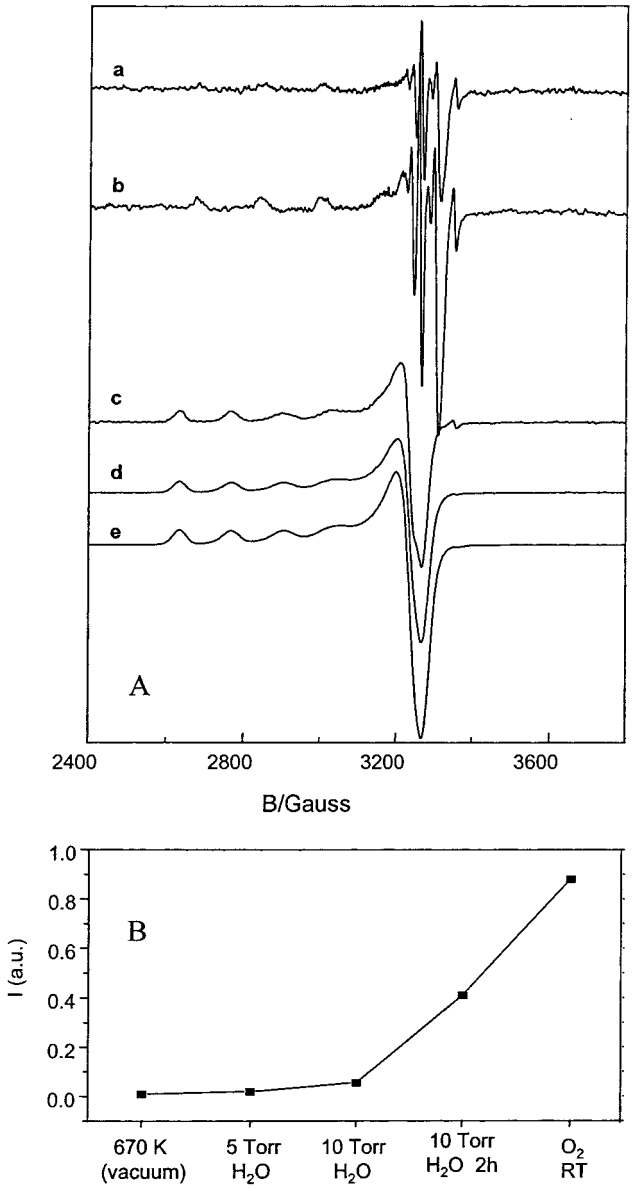

Figure 6. EPR spectra (A) and corresponding intensities (B) of Cu/ZSM-5 rehydrated at room temperature with progressively increasing doses of water. The final spectrum (e) is related to the interaction with O_2 at room temperature of the rehydrated sample.

Water vapor not only has the effect of increasing the EPR spectral intensity of Cu^{2+} but also changes the conditions for oxidation by molecular oxygen. If O_2 is adsorbed (at room temperature) on the sample after preliminarly contact with water, a further relevant growth of the signal intensity is observed, which is documented by the last spectrum in Figure 6A and by the corresponding intensity value in Figure 6B. The final intense spectrum (very close to the initial intensity) maintains the same shape (typical of hydrated cupric ions) as those recorded after water contact. The partial rehydration of the system is thus the condition for observing an efficient oxidative effect of molecular oxygen even at room temperature. In this case our data agree with those of Kasai and Bishop, who reported the same phenomenon on Cu−Mordenite.[57] As the role of consecutive dosing of water and oxygen onto dehydrated materials seems to be critical, we have followed this process by the other spectroscopic techniques to complement the information derived from EPR.

3.2.2. IR and Vis−Near-IR Spectroscopies. The effect on the 980 cm^{-1} band, characteristic of Cu^{+}/ZSM-5, of water adsorption at room temperature and of the subsequent oxygen adsorption is illustrated in Figure 7A. Upon interaction with water the disappearance of the typical band ascribed to the ν_{asym}(SiOAl) perturbed by Cu^{+} species at 980 cm^{-1} is observed (see Figure 2A, curve b). This fact can be interpreted considering the solvation effect of water which moves the copper ions away from the zeolite walls. Upon water-excess removal and subsequent oxygen dosage at room temperature (curve c of Figure 7A), the spectrum typical of Cu^{2+} species (band at about 920 cm^{-1}) is completely restored.

Parallel results are found following the same experiment by Vis−near-IR spectroscopy. In Figure 7B the spectra obtained for the "as-prepared" material (curve d) and for 670 K dehydrated Cu^{2+}/ZSM-5 (curve a) are compared with the spectra obtained upon consecutive interaction of the latter sample with H_2O (curve b) and with O_2 (curve c) at room temperature. It has to be noticed that the interaction with water (curve b) is

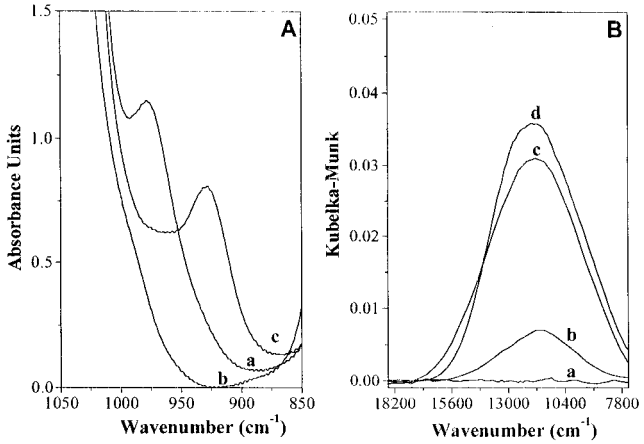

Figure 7. (A) Evolution of the IR spectra in the 1050−850 cm^{-1} range upon interaction with adsorbates. Sample activated at 673 K (curve a), after interaction with H_2O (curve b) and subsequent O_2 dosage (curve c). (B) Evolution of the vis−near-IR spectra, in the d−d region, curves a−c as in part A. Curve d reports the spectrum obtained on the fresh sample activated at 300 K for comparison.

actually accompanied by the formation of a weak absorption typical of Cu^{2+}, indicating the onset of a limited oxidation upon water adsorption. A thorough oxidation of cuprous ions, however, is observed only after O_2 interaction with the rehydrated sample (curve C), which definitely restores most of the original $Cu^{2+}(H_2O)_n$ band. The origin of the weak oxidation by water is still unclear and should probably be searched in the presence of traces of molecular oxygen in the liquid water reservoir.

3.2.3. XAFS. As documented in Figure 8A, the in situ dosage of H_2O leaves nearly unaffected the 8983 eV peak of the EXAFS spectrum, confirming that pure water is not effective in the oxidation of Cu^+ ions in ZSM-5 at RT. On the contrary, the subsequent dosage of O_2 has a dramatic effect on the Cu^+ preedge peak, which is reduced at about one-third of its original magnitude. In the upper inset the weak 1s → 3d absorption of Cu^{2+} species is again visible at about 8977.0 eV. Since the XANES region of the X-ray absorption spectrum represents the linear average of all the copper species available in the sample, weighted by the corresponding abundance (i.e., no XANES silent species can be hypothesized), it can thus be concluded, in agreement with IR and UV data, that the amount of reoxidized Cu^+ species after interaction with pure water vapor is negligible, while it is consistent after successive interaction with oxygen.

The interaction with H_2O and H_2O/O_2 mixture is also reported reported in Figures 8B (EXAFS) and 9 in *k* and *r* space, respectively. In both cases the ligand dosage strongly modifies the first coordination shell around the cuprous species, as documented by the strong variation in both the period and intensity of the $\chi(k)$ oscillations, at 1.5−6.0 $Å^{-1}$. This observation, combined with the previously discussed XANES data (Figure 8A), is particularly relevant since, for the dosage of pure water, it proves that even if H_2O molecules are able to penetrate within the Cu^+ first coordination shell, they are not able to change the oxidation state of cuprous cations.[58]

Figure 9 indicates that the dosage of H_2O also has an effect on the Cu−O−Cu dimers ($[Cu-O-Cu]^+$ oxocations). Of particular relevance is the strong reduction of the dimer peak at about 2.4 Å obtained after interaction with pure water at RT: EXAFS spectroscopy clearly indicates a partial disaggregation of Cu−O−Cu dimers, which could explain the increase of the EPR signal observed after dosage of H_2O.

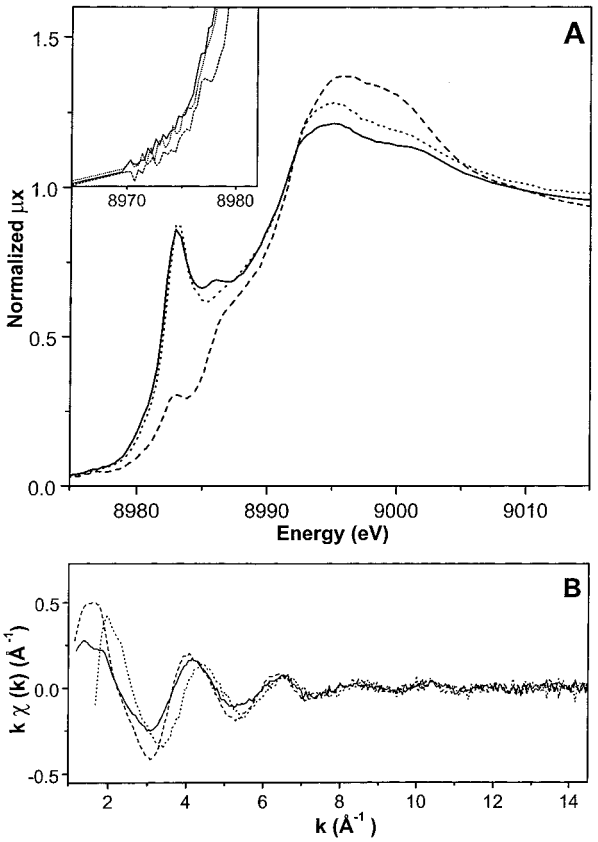

Figure 8. (A) XANES spectra of Cu^{II}/ZSM-5 thermally treated at 673 K (full line) and after interaction with H_2O (dotted line) and subsequent O_2 dosage (dashed line). The inset in the upper left corner reports the magnification of the 1s → 3d electronic transition. (B) As part A for the experimental $k\chi(k)$ spectra (averaged over three acquisitions).

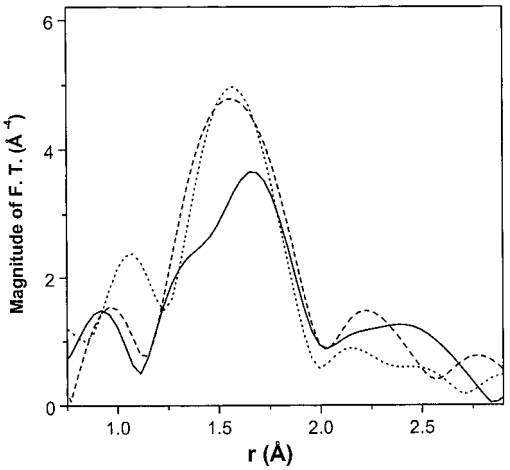

Figure 9. k^3-weighted FT of EXAFS data reported in Figure 8B (lines with the same drafts in Figure 8B).

3.3. Mechanism of Reduction−Reoxidation of Copper Ions in ZSM-5. The results reported in the previous sections can be summarized as follows.

(a) Dehydration treatments under vacuum of Cu^{2+} exchanged ZSM-5 samples cause a dramatic decrease of Cu^{2+} EPR spectra intensity starting from relatively low dehydration temperatures till 673 K (Figure 1).

(b) In the range 300−473 K the decrease of EPR spectral intensity is not accompanied by Cu^+ formation, but only by modifications in the coordination sphere of Cu^{2+} ions. Reduction of Cu^{2+}, as documented by IR, Vis−near-IR, and XANES data,

becomes effective at $T > 473$ K and is dominant in the range 473−673 K (Figures 2, 3A, and 4).

(c) The samples dehydrated at 673 K and mainly containing Cu^+ are not oxidized by molecular oxygen at room temperature. However, by oxidation in "dry" conditions at 673 K intense EPR spectra of Cu^{2+} are given whose intensity represents about 40% of the intensity of the starting materials assumed as a reference (Figure 5).

(d) Water adsorption at room temperature on dehydrated reduced materials (Figure 6, spectra a−d) is capable of causing an increase of the EPR signal intensity comparable to that obtained by oxygen at 670 K (about 40% of the initial signal) but does not cause the appearance (except for minor features) of the typical manifestations of Cu^{2+} ions in the infrared, Vis−near-IR, and XANES.

(e) On the rehydrated samples, adsorption of oxygen causes a net increase of the EPR intensity for simple adsorption at room temperature (Figure 6, spectrum e) so that the original intensity of the hydrated material is practically recovered. This is accompanied by a strong reduction of Cu^+ features in the XANES spectrum (Figure 8) and by the recovery of Cu^{2+} features in the infrared and Vis−near-IR spectroscopies (Figure 7).

Points a and b are in contrast with the recently proposed mechanism[25] involving cupric ion reduction along the dehydration process (eq 4)[25] since, in that case, the formation of Cu^+ and $Cu^{2+}O^-$ should be simultaneous starting from the early stages of dehydration. The data reported here are instead in agreement with the results reported by Lo Jacono et al.,[26] indicating that the magnetic susceptibility of the solid (related to the presence of Cu^{2+}) is constant in the range 298−473 K of dehydration temperature. We are thus in favor of a dehydration mechanism in two steps. In the former one the loss of water is accompanied by a rearrangement of the cupric ion coordination involving formation of EPR silent species.

Defining the features of these silent species is not straightforeword. Three main limiting hypotheses have in principle to be considered and are described as follows, but the problem remains currently under investigation in our laboratory.

(a) The presence of isolated paramagnetic Cu^{2+} in some particular low coordination state characterized by very fast relaxation. Conesa and Soria, for instance,[59] explained some drop of the EPR intensity in Cu^{2+}/Y zeolites, hypothesizing the formation, induced by dehydration of the solid, of cupric ions in C_{3v} trigonal symmetry slightly distorted by Jahn−Teller effects. The perfect trigonal coordination involves a degenerate ground state, and the distortion should be low enough to generate a low-lying excited state with a consequent short relaxation time, and large line broadening, for the spin system.

(b) The presence of $Cu^{2+}O^{2-}Cu^{2+}$ diamagnetic pairs ($S = 0$, antiferromagnetic coupling between the two spins). The existence of such pairs or even of small copper−oxygen clusters in Cu/ZSM-5 has been reported in the past by several authors[16,60] and has been confirmed by XAFS data of the present work (section 1).

(c) The presence of $Cu^{2+}O^{2-}Cu^{2+}$ ferromagnetic pairs ($S = 1$) having very large zero field splitting because of strong distortion in the symmetry. In this case the spin transitions should be out of the field region covered by the X band experiment in the EPR.

It is impossible, on the basis of the present data, to unambiguously clarify whether the state of copper in dehydrated ZSM-5 corresponds with one or more of the previous hypotheses. It can be observed however that the hypotheses in (a) and (c) are in agreement with the constancy of the magnetic susceptibility during dehydration,[26] while those in (b) and (c) are compatible with the presence of extralattice oxygen (ELO) and with the mechanism proposed for the copper reduction at $T > 473$ K based on ELO depletion (vide infra). On the other hand, the hypothesis in (b) is in line with the behavior of cupric oxide which is, in fact, antiferromagnetic. In the following discussion we will maintain the idea of the presence of both low coordinated isolated copper ions (Cu^{2+}_{LC}) and of copper pairs as the possible states for EPR silent cupric species without further specification.

The second step of dehydration starts at a temperature of about 473 K and is dominated by the reduction of Cu^{2+} ions to Cu^+. The $Cu^{2+}O^{2-}Cu^{2+}$ pairs are mainly involved in the process together with the isolated (EPR visible) cupric ions, a fraction of which (Figure 1 spectra b−c) are probably reduced passing from 473 to 673 K of dehydration temperature. The formation of Cu^+ in the dehydrated Cu/ZSM-5 is not substantially questioned, and the related evidence presented in this and other papers is clear and unambiguous. As to the mechanism of Cu^+ formation, the hypothesis of oxygen depletion from the solid with consequent reduction of cupric ions (eq 1) seems the more likely one. Oxygen depletion does not involve, of course, the zeolitic framework but those oxygen atoms introduced in the zeolite during the exchange reaction as hydroxyl groups and then transformed upon dehydration into the so-called ELO species which are, according to Keith Hall,[23] easily desorbed at high temperature as molecular oxygen. The ELO depletion is, by the way, in line with the chemistry of copper oxide and of several semiconducting oxides easily reducible by thermal treatment under vacuum. Oxygen evolution from Cu/ZSM-5 or Cu−Mordenite has been indeed observed and quantitatively measured by various authors in the past.[23,57] The particular trend of Cu^{2+} EPR spectrum intensities involving, in the context of a general decrease of spectral intensity along dehydration, some relatively small increase of the intensity for $T > 473$ K (Figure 1) also observed by Larsen et al.[25] and LoJacono et al.[26] can be explained considering the complex interplay between the already described process leading to aggregation of cupric ions in paramagnetic assemblies and the opposite process driven by the temperature and leading to ion migration and to a partial redispersion of the cupric ions in isolated zeolitic sites. The whole picture proposed above is schematically reported in Figure 10. This figure illustrates the described chemical processes as a function of the temperature of the thermal treatment. The starting state of the sample is reported in terms of hydrated $Cu^{2+}OH^-$ species as it is well-known that in a wide range of pH[5−8,26] the ion exchange leads to this kind of hydroxylated cupric species. Figure 10 does not report (for the sake of clarity) the effect of molecular oxygen at 673 K on the dehydrated samples, which consists of the oxidation to Cu^{2+} of a consistent fraction of the whole copper present as Cu^+ (about 40%). The fact that the oxidation in such conditions does not involve the whole copper present in the sample indicates that part of the copper itself, though not visible in terms of EPR on the dehydrated sample (Figure 5), is still in the oxidized Cu^{2+} state (left-hand part of Figure 10).

The effects of water adsorption at room temperature on dehydrated reduced samples constitute the most original results of the present work and are summarized by points d and e at the beginning of this section and are illustrated in Figure 11. The starting point of this figure corresponds to the final situation of Figure 10. The increase of the EPR intensity caused by water at room temperature is complementary to the effect of oxygen

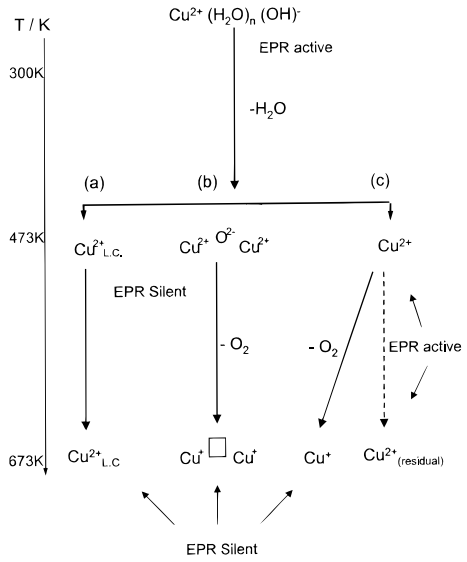

Figure 10. Schematic description of the effects of thermal treatment under vacuum on Cu/ZSM-5 as a function of the temperature.

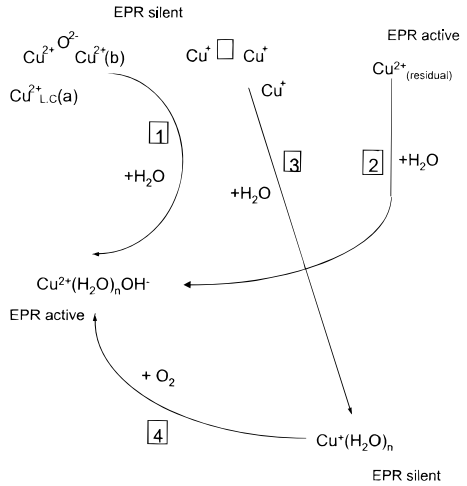

Figure 11. Effect of rehydration at room temperature on the various species produced by dehydrating thermal treatment (see Figure 10). The effect of molecular oxygen at room temperature on the rehydrated sample is also reported (step 4).

at 773 K in that it involves that fraction of EPR silent Cu^{2+} ions which is present in the sample after thermal treatment (reaction 1 in Figure 11). The effect of water is of generating a more symmetric ligand shell around the isolated poorly coordinated Cu^{2+} ions (Figure 11, species a) and, in the meantime, of dispersing the silent residual aggregates of cupric ions (species b) so that all the ions involved in this interaction become again EPR visible and assume the typical spectral shape recorded for the starting materials. All the described rehydration process (Figure 6, spectra b−d) occurs without substantial oxidation of Cu^{+} ions as indicated by both IR and XANES results (Figures 7A and 8A). The latter technique in particular indicates that water modifies the coordination sphere of Cu^{+} but not its oxidation state. The present finding, on one hand, does not agree with the scheme proposed in ref 25 and reported in eq 4 in which water adsorption ensures the reoxidation of Cu^{+} ions to Cu^{2+}. On the contrary they are in agreement with data by Kasai and Bishop[57] who found, for Cu^{2+} exchanged mordenite, that oxygen is released by the sample upon treatment in vacuo at $T > 570$ K and that carefully purified, oxygen free, water is not able to oxidize cuprous ions to cupric ones. This latter fact was explained by the authors in terms of redox

SCHEME 1

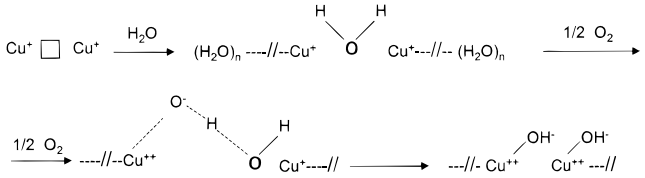

potentials. The potential for the semireaction is too low to allow

$$Cu^{+} \rightarrow Cu^{2+} + e^{-} \quad (E^{\circ} = -0.158 \text{ V})$$

oxidation (of Cu^{+}) by water. When this latter process takes place (as in the case of the Cr^{2+}/Cr^{3+} pair, $E^{\circ} = +0.41$), this occurs with reduction of water and molecular hydrogen is released in the gas phase.

The data reported in the present paper nicely agree with those of Kasai and Bishop also for the fact reported in point e at the beginning of this section, i.e., for the synergistic cooperation between water and oxygen to allow cuprous ion oxidation at room temperature. Oxidation by molecular oxygen, as shown in point c, does not take place in a dry environment but easily occurs when water is admitted into the system prior to O_2 adsorption. In such conditions incorporation of oxygen into the system can take place, and in parallel, Cu^{+} is oxidized to Cu^{2+} (reaction 4 in Figure 11).

The reason for this phenomenon can probably be found in the different energy barriers needed for oxygen reduction and oxygen incorporation in the two cases. Keeping in mind that the whole electrostatic balance in the zeolitic framework must be conserved in all stages of the system evolution and that a single positive charge is associated with each cupric ion introduced by ion exchange as $Cu^{2+}OH^{-}$ ions, the following points can be inferred.

(i) In a dry environment incorporation of oxygen (ELO) must occur via stepwise one-electron reduction of O_2 by cuprous ions.

(ii) Preadsorption of water and consequent rehydration of the system probably allows the reoxidation to follow a less activated (or nonactivated) pathway, directly leading to the same type of copper species present in the as-prepared material. A hypothesis of the oxidation mechanism could thus be that given in Scheme 1.

A somehow similar mechanism was proposed by Kasai and Bishop,[57] who suggested a role of zeolitic hydroxyl groups in assisting cuprous ion oxidation with a chemistry similar to that expected for Cu^{+} in acidic oxygenated aqueous media. In the whole process of rehydration−reoxidation reported in Figure 11, the reactions are schematically illustrated without the details of the previous scheme.

4. Conclusions

The present investigation has put into evidence some basic points which should be useful to define the state of copper in ZSM-5 zeolites upon various types of treatment. They can be described as follows.

(a) The first part of the thermal treatment on hydrated Cu^{2+}/ZSM-5 (between RT and 473 K) essentially involves water elimination (without substantial Cu^{2+} reduction) and reorganization of cupric ions, a fraction of which become EPR silent.

(b) Reduction of cupric ions occurs beyond 473 K with oxygen elimination and Cu^{+} formation, whose presence is evidenced by a variety of spectroscopic techniques.

(c) Oxidation by molecular oxygen in a dehydrated environment is an activated process and does not occur at room temperature.

(d) Interaction with water at room temperature does not cause oxidation of the system, and the increase, in such conditions, of the EPR spectra intensity is related to dispersion and coordination of previously silent Cu^{2+} species. A second role of water, however, is to facilitate the reoxidation of the system by molecular oxygen assisting reoxidation probably via some acid−base mechanism.

Acknowledgment. The present work is part of a project coordinated by A. Zecchina and cofinanced by the Italian MURST (Cofin 98, Area 03). G.T.P. is thankful to the European Community for a TMR grant.

References and Notes

(1) Nicula, A.; Stamires, D.; Turkevich, J. *J. Chem. Phys.* **1965**, *42*, 3684.
(2) Richardson, J. T. *J. Catalysis* **1967**, *9*, 178.
(3) Dempsey, E.; Olson, D. H. *J. Chem. Phys.* **1970**, *74*, 178.
(4) Chao, C. C.; Lunsford, J. H. *J. Chem. Phys.* **1972**, *57*, 2890.
(5) Iwamoto, M.; Furukawa, H.; Mine, Y.; Uemura, F.; Mikuriya, S.; Kagawa, S. *J. Chem. Soc., Chem. Commun.* **1986**, 1272.
(6) Iwamoto, M.; Yahiro, H.; Mine, Y.; Kagawa, S. *Chem. Lett.* **1989**, 213.
(7) Iwamoto, M.; Yahiro, H.; Kutsuno, T.; Bunyo, S.; Kagawa, S. *Bull. Chem. Soc. Jpn.* **1989**, *62*, 583.
(8) Iwamoto, M.; Yahiro, H.; Tanda, K.; Mizuno, N.; Mine, Y.; Kagawa, S. *J. Phys. Chem.* **1991**, *95*, 3727.
(9) Iwamoto, M.; Yahiro, H.; Mizuno, K. N.; Zhang, Y. W. X.; Mine, Y.; Kagawa, S. *J. Phys. Chem.* **1992**, *96*, 9360.
(10) Yamashita, H.; Matsuoka, M.; Tsuji, K.; Shioya, Y.; Anpo, M.; Che, M. *J. Phys. Chem.* **1996**, *100*, 397.
(11) Hamada, H.; Matsubayashi, N.; Shimada, H.; Kintaichi, Y.; Ito, T.; Nishijima, A. *Catal. Lett.* **1990**, *5*, 189.
(12) Grünert, W.; Hayes, N. W.; Joyner, R. W.; Shpiro, E. S.; Rafiq, M.; Siddiqui, H.; Baeva, G. N. *J. Phys. Chem.* **1994** *98*, 10832.
(13) Kharas, K. C. C. *Appl. Catal. B* **1993**, *2*, 207.
(14) Liu, D.-J.; Robota, H. J. *Appl. Catal. B* **1994**, *4*.
(15) Kharas, K. C. C.; Liu, D.-J.; Robota, H. J. *Catal. Today* **1995**, *26*, 129.
(16) Beutel, T.; Sàrkàny, J.; Lei, G.-D.; Yan, J. Y.; Sachtler, W. M. H. *J. Phys. Chem.* **1996**, *100*, 845.
(17) Lamberti, C.; Bordiga, S.; Salvalaggio, M.; Spoto, G.; Zecchina, A.; Geobaldo, F.; Vlaic, G.; Bellatreccia, M. *J. Phys. Chem. B* **1997**, *101*, 344.
(18) Kumashiro, R.; Kuroda, Y.; Nagao, M. *J. Chem. Phys. B* **1999**, *103*, 89.
(19) Li, Y.; Keith Hall, W. *J. Catal.* **1991**, *129*, 202.
(20) Sàrkàny, J.; d'Itri, J. L.; Sachtler, W. M. H. *Catal. Lett.* **1992**, *16*, 241.
(21) Keith Hall, W.; Vaylon, J. *Catal. Lett.* **1992**, *15*, 311.
(22) Valyon, J.; Keith Hall, W. *J. Phys. Chem.* **1993**, *97*, 7054.
(23) Jong, H. J.; Keith Hall, W.; d'Itri, J. L. *J. Phys. Chem.* **1996**, *100*, 9416.
(24) Cheung, T.; Bhargava, S. K.; Mobday, M.; Foger, K. *J. Catal.* **1996**, *158*, 301.
(25) Larsen, S. C.; Aylor, A.; Bell A.; Reimer, J. A. *J. Phys. Chem.* **1994**, *98*, 11533.
(26) Lo Jacono, M.; Fierro, G.; Dragone, R.; Feng, X.; d'Itri, J.; Keith Hall, W. *J. Phys. Chem. B* **1997**, *101*, 1979.
(27) Pascarelli, S.; Boscherini, F.; D'Acapito, F.; Meneghini, C.; Hrdy J.; Mobilio, S. *J. Synchrotron Radiat.* **1996**, *3*, 147.
(28) Bordiga, S.; Zecchina, A.; Lamberti, C.; Salvalaggio, M.; Spoto, G.; D'Acapito, F. *ESRF Proposal CH-542*; BM8 GILDA beamline, 10/10−14/1998.
(29) Lytle, F. W.; Sayers, D. E.; Stern, E. A. *Physica B* **1989,** *158*, 701.
(30) Lengeler, B.; Eisenberger, P. *Phys. Rev. B* **1980**, *21*, 4507.
(31) Michalowicz, A. *J. Phys. IV France* **1997,** *7*, C2−235.
(32) Anderson, M. W.; Kevan, L. *J. Phys. Chem.* **1987**, *91*, 4174.
(33) Kucherov, A. V.; Slinkin, A. A. *J. Phys. Chem.* **1989**, *93*, 864.
(34) Schoonheydt, R. *Catal. Rev.* **1993**, *35*, 129.
(35) Giamello, E.; Murphy, D.; Magnacca, G.; Morterra, C.; Shioya, Y.; Nomura, T.; Anpo, M. *J. Catal.*, **1992**, *136*, 510.
(36) Sojka, Z.; Che, M.; Giamello, E. *J. Phys. Chem.* **1997**, *101*, 4831.
(37) Scarano, D.; Zecchina, A.; Bordiga, S.; Geobaldo, F.; Spoto, G.; Petrini, G.; Leofanti, G.; Padovan, M.; Tozzola, G. *J. Chem. Soc., Faraday Trans*. **1993**, *89*, 4123.
(38) Zecchina, A.; Bordiga, S.; Scarano, D.; Lamberti, C.; Ricchiardi, G. Petrini, G. Leofanti G. and Mantegazza, M. *Catal. Today* **1996**, *32*, 97.
(39) Bordiga, S.; Buzzoni, R.; Geobaldo, F.; Lamberti, C.; Giamello, E.; Zecchina, A.; Leofanti, G.; Petrini, G.; Tozzola, G.; Vlaic, G. *J. Catal.* **1996**, *158*, 486.
(40) Sobalik Z.; Tvarenzkova Z.; Wichterlowa, B. *J. Phys. Chem. B* **1998**, *102*, 1077.
(41) Sarkany, J. *J. Mol. Struct.* **1997**, *410*, 95.
(42) Sarkany, J.; Sachtler, W. M. H. *Zeolites* **1994**, *14*, 7.
(43) Zecchina, A.; Bordiga, S.; Turnes Palomino, G.; Scarano, D.; Lamberti, C.; Salvalaggio, M. *J. Phys. Chem. B* **1999**, *103*, 3833.
(44) Figgis, B. N. *Introduction to ligand field*; Interscience Publishers: New York, 1966.
(45) Wilkinson, G. *Comprehensive coordination chemistry*; Pergamon Press: Oxford, U.K., 1987; Vol. 5.
(46) Friedman, R. M.; Freeman, J. J.; Lytle, F. W. *J. Catal.* **1978,** *55***,** 10.
(47) Tranquada, J. M.; Heald, S. M.; Moodenbaugh, A. R. *Phys. Rev. B* **1987**, *36*, 5263.
(48) Kau, L. S.; Spira-Solomon, D. J.; Penner-Hahn, J. E.; Jodgson, K. O.; Solomon, E. I. *J. Am. Chem. Soc.* **1987**, *109*.
(49) Blackburn, N. J.; Strange, R. W.; Reedijk, J.; Volbeda, A.; Farooq, A.; Karlin, A.; Zubieta, J. *Inorg. Chem.* **1989**, *28*, 1349.
(50) Blackburn, N. J.; Hasnain, S. S.; Pettigrill, T. M.; Strange, R. W.; Reedy, B. J.; Blackburn, N. J. *J. Am. Chem. Soc.* **1994**, *116*, 1924.
(51) Kuroda, Y.; Yoshikawa, Y.; Konno, S.; Hamano, H.; Maeda, H.; Kumashiro, R.; Nagao, M. *J. Phys. Chem.* **1995**, *99*, 10621.
(52) Kuroda, Y.; Maeda, H.; Yoshikawa, Y.; Kumashiro, R.; Nagao, M. *J. Phys. Chem. B* **1997**, *191*, 1321.
(53) Kuroda, Y.; Kotani, A.; Maeda, H.; Moriwaki, H.; Morimato, T.; Nagao, M. *J. Chem. Soc., Faraday Trans.* **1992**, *88*, 1583.
(54) Yamashita, H.; Matsuoka, M.; Tsuji, K.; Shioya, Y.; Anpo, M.; Che, M. *J. Phys. Chem.* **1996**, *100*, 397.
(55) Lamberti, C.; Spoto, G.; Scarano, D.; Pazé, C.; Salvalaggio, M.; Bordiga, S.; Zecchina, A.; Turnes Palomino G.; D'Acapito, F. *Chem. Phys. Lett.* **1997**, *269*, 500.
(56) Grünert, W.; Hayes, N. W.; Joyner, R. W.; Shpiro, E. S.; Rafiq, M.; Siddiqui, H.; Baeva, G. N. *J. Phys. Chem.* **1994**, *98*, 10832.
(57) Kasai P. H.; Bishop, R. J. *J. Phys. Chem.* **1977**, *81*, 1527.
(58) It is worth noticing that, at higher k values (6.0−13 $Å^{-1}$ interval), the $\chi(k)$ function is much less affected by ligand dosage. This fact can be explained in terms of a weak interaction of water and H_2O/O_2 molecules to copper species, giving rise to a Cu−adsorbate distance affected by a large Debye−Waller factor, which in turn implies a reduction of the EXAFS signal coming from adsorbates particularly consistent at high k values, where the contribution of the framework oxygens becomes largely predominant.
(59) Conesa, J. C.; Soria, J. *J. Phys. Chem.* **1978**, *82*, 1847.
(60) Sarkany, J.; d'Itri, J. L.; Sachtler, W. M. H. *Catal. Lett.* **1992**, *16*, 241.